International Journal of Modern Physics B
Vol. 23, No. 5 (2009) 703–710

World Scientific
www.worldscientific.com

STOCHASTIC SPIKING COHERENCE IN COUPLED SUBTHRESHOLD MORRIS-LECAR NEURONS

WOOCHANG LIM
Neuroscience Laboratory, Institute for Medical Sciences,
Ajou University School of Medicine, Suwon 443-721, Korea
wclim@kangwon.ac.kr

SANG-YOON KIM*
Department of Physics, Kangwon National University,
Chunchon, Kangwon-Do 200-701, Korea
sykim@kangwon.ac.kr

Received 17 November 2008

We consider a large population of globally coupled subthreshold Morris-Lecar neurons. By varying the noise intensity D, we numerically investigate stochastic spiking coherence (i.e., collective coherence between noise-induced neural spikings). As D passes a lower threshold, a transition from an incoherent to a coherent state occurs because of a constructive role of noise to stimulate coherence between noise-induced spikings. However, when passing a higher threshold of D, another transition from a coherent to an incoherent state takes place due to a destructive role of noise to spoil the spiking coherence. Such an incoherence-coherence-incoherence transition is well-described in terms of the order parameter which is just the mean square deviation of the global potential. In the coherent regime, we also characterize the degree of stochastic spiking coherence by using a coherence measure which reflects the degree of "resemblance" of the global potential to the local potential. Thus, stochastic spiking coherence with large coherence measure is found to occur over a large range of intermediate noise intensity.

Keywords: Stochastic spiking coherence; coupled subthreshold Morris-Lecar neurons.

PACS numbers: 87.19.L-, 05.40.Ca

1. Introduction

In recent years, there has been great interest in brain rhythms.[1] Synchronous oscillations in neural systems are correlated with neural encoding of sensory stimuli (e.g., binding of the integrated whole image in the visual cortex is accomplished via synchronization of neural firings).[2] Population dynamics has been intensively investigated in coupled systems, consisting of spontaneously firing (self-oscillating)

*Corresponding author.

neurons, and thus three types of mechanisms for neural synchronization have been found.[3] In this paper, we are interested in noise-induced coherent dynamics in neural networks, composed of subthreshold neurons. (Each subthreshold neuron in the absence of coupling cannot fire spontaneously without noise; it can fire only with the help of noise.) Counterintuitively, noise sometimes plays a constructive role in the emergence of dynamical order. A distinguished example of such manifestations is the stochastic resonance through which noise-enhanced detection of weak signal can occur.[4] Recently, much attention has been paid to noise-induced coherence in coupled excitable systems.[5]

This paper is organized as follows. In Sec. 2, we consider a large ensemble of globally coupled subthreshold Morris-Lecar (ML) neurons.[6–8] By varying the noise intensity D, we numerically investigate stochastic spiking coherence (i.e., collective coherence between noise-induced neural spikings) for a fixed coupling strength. For small D, neurons fire independently, and hence the global output signal (i.e., the ensemble-averaged membrane potential) becomes incoherent. However, as D passes a lower threshold, the global output signal becomes coherent (i.e., it exhibits a collective motion on a noisy limit cycle) due to a constructive role of noise to stimulate coherence between noise-induced spikings. When D is large, noise spoils spiking coherence, and a complete loss of stochastic spiking coherence occurs when passing a higher threshold. As in globally coupled chaotic systems,[9–12] this incoherence-coherence-incoherence transition may be well-described in terms of the order parameter which is just the mean square deviation of the global output signal. In the coherent regime, we also characterize the degree of stochastic spiking coherence by using a coherence measure M which reflects the degree of "resemblance" of the global potential to the local potential. As D passes the lower threshold, M increases dramatically at first, showing onset of coherence, then it becomes nearly constant large over a wide range of D, and for large D, it decreases due to the destructive role of noise to spoil the spiking coherence. Thus, stochastic spiking coherence with large M is found to occur over a large range of intermediate noise intensities. Finally, a summary is given in Sec. 3.

2. Stochastic Spiking Coherence in Globally Coupled Subthreshold ML Neurons

We consider a large ensemble of N globally coupled ML neurons.[6–8] The population dynamics in this neural network is governed by the following differential equations:

$$C\frac{dV_i}{dt} = -I_{\text{ion},i} + I_{\text{DC}} + D\xi_i + I_{\text{syn},i}, \tag{1a}$$

$$\frac{dw_i}{dt} = \phi\frac{(w_\infty(V_i) - w_i)}{\tau_R(V_i)}, \quad i = 1, \ldots, N, \tag{1b}$$

where

$$I_{\text{ion},i} = I_{\text{Ca},i} + I_{K,i} + I_{L,i} \tag{2a}$$

$$= g_{\rm Ca} m_\infty(V_i)(V_i - V_{\rm Ca}) + g_K w_i (V_i - V_K) + g_L (V_i - V_L)\,, \tag{2b}$$

$$I_{{\rm syn},i} = \frac{J}{N-1} \sum_{j(\neq i)}^{N} \Theta(V_j - V^*)\,, \tag{2c}$$

$$m_\infty(V) = 0.5[1 + \tanh\{(V - V_1)/V_2\}]\,, \tag{2d}$$

$$w_\infty(V) = 0.5[1 + \tanh\{(V - V_3)/V_4\}]\,, \tag{2e}$$

$$\tau_R(V) = 1/\cosh\{(V - V_3)/(2V_4)\}\,. \tag{2f}$$

Here, the state of the ith neuron at a time t (measured in units of ms) is characterized by the membrane potential V_i (measured in units of mV) and the slow recovery variable w_i representing the activation of the K^+ current (i.e., the fraction of open K^+ channels). C in Eq. (1a) represents the capacitance of the membrane of each neuron, and the time evolution of V_i is governed by four kinds of source currents.

The total ionic current $I_{{\rm ion},i}$ of the ith neuron is composed of the calcium current $I_{{\rm Ca},i}$, the potassium current $I_{K,i}$, and the leakage current $I_{L,i}$. Each ionic current obeys the Ohm's law. The constants $g_{\rm Ca}$, g_K, and g_L are the maximum conductances for the ion and leakage channels, and the constants $V_{\rm Ca}$, V_K, and V_L are the reversal potentials at which each current is balanced by the ionic concentration difference across the membrane. Since the calcium current $I_{{\rm Ca},i}$ changes much faster than the potassium current $I_{K,i}$, the gate variable m_i for the Ca^{2+} channel is assumed to always take its saturation value $m_\infty(V_i)$. On the other hand, the activation variable w_i for the K^+ channel approaches its saturation value $w_\infty(V_i)$ with a relaxation time $\tau_R(V_i)/\phi$, where τ_R has a dimension of ms and ϕ is a (dimensionless) temperature-like time scale factor.

Each ML neuron is also stimulated by the common DC current $I_{\rm DC}$ and an independent Gaussian white noise ξ [see the second and third terms in Eq. (1a)] satisfying $\langle \xi_i(t) \rangle = 0$ and $\langle \xi_i(t)\ \xi_j(t') \rangle = \delta_{ij}\ \delta(t - t')$, where $\langle \cdots \rangle$ denotes the ensemble average. The noise ξ_i is a parametric one which randomly perturbs the strength of the applied current $I_{\rm DC}$, and its amplitude is controlled by the parameter D. The last term in Eq. (1a) represents the synaptic coupling of the network. Each neuron is connected to all the other ones through global instantaneous pulse-type synaptic couplings. $I_{{\rm syn},i}$ of Eq. (2c) represents such a synaptic current injected into the ith neuron. The coupling strength is controlled by the parameter J, $\Theta(x)$ is the Heaviside step function (i.e., $\Theta(x) = 1$ for $x \geq 0$ and $\Theta(x) = 0$ for $x < 0$), and V^* is the threshold value for the spiking state (i.e., for $V_i > V^*$ a local spiking state of the ith neuron appears). Here, we consider the excitatory coupling of $J > 0$ and set $V^* = 0$ mV.

The ML neuron may exhibit either type-I or type-II excitability, depending on the system parameters. In this paper, we consider the case of type-II excitability

where $g_{\rm Ca} = 4.4$ mS/cm^2, $g_K = 8$ mS/cm^2, $g_L = 2$ mS/cm^2, $V_{\rm Ca} = 120$ mV, $V_K = -84$ mV, $V_L = -60$ mV, $C = 5$ μF/cm^2, $\phi = 0.04$, $V_1 = -1.2$ mV, $V_2 = 18$ mV, $V_3 = 2$ mV, and $V_4 = 30$ mV.[13] As $I_{\rm DC}$ passes a threshold in the absence of noise, each single type-II ML neuron begins to fire with a nonzero frequency which is relatively insensitive to the change in $I_{\rm DC}$.[14,15] Numerical integration of Eq. (1) is done using the Heun method[16] (with the time step $\Delta t = 0.01$ ms) similar to the second-order Runge-Kutta method, and data for (V_i, w_i) $(i = 1, \ldots, N)$ are obtained with the sampling time interval $\Delta t = 1$ ms. For each realization of the stochastic process in Eq. (1), we choose a random initial point $[V_i(0), w_i(0)]$ for the ith $(i = 1, \ldots, N)$ neuron with uniform probability in the range of $V_i(0) \in (-60, 60)$ and $w_i(0) \in (0.1, 0.5)$.

We consider a subthreshold case of $I_{\rm DC} = 84$ μA/cm^2. For an isolated single case, each subthreshold neuron cannot fire spontaneously in the absence of noise, and it may generate firings only with the aid of noise. We set $J = 50$ μA/cm^2 and numerically investigate stochastic spiking coherence (i.e., collective coherence between noise-induced firings) by varying the noise amplitude D for $N = 10^3$. Emergence of global spiking coherence in the ensemble may be described by the global potential $V_G(t)$ (i.e., the population-averaged membrane potential) and the global recovery variable $W_G(t)$,

$$V_G(t) = \frac{1}{N}\sum_{i=1}^{N} V_i(t) \quad \text{and} \quad W_G(t) = \frac{1}{N}\sum_{i=1}^{N} w_i(t)\,. \tag{3}$$

For sufficiently small D, neurons fire independently, and hence incoherent states appear. For an incoherent case of $D = 0.1$ μA$\cdot$ms$^{1/2}$/cm^2, the phase portrait of the global state (V_G, W_G) and the time series of the global potential $V_G(t)$ are shown Figs. 1(a) and 1(b), respectively. The global state lies at a noisy equilibrium point, and the global potential $V_G(t)$ is nearly stationary. However, as D passes a lower threshold D_l^* ($\simeq 0.115$ μA$\cdot$ms$^{1/2}$/cm^2) a coherent transition occurs because noise stimulates collective coherence between neural spikings. Then, stochastic spiking coherence occurs, as shown in Figs. 1(c) and 1(d) for $D = 0.3$ μA$\cdot$ms$^{1/2}$/cm^2. For this coherent case, the global state exhibits a counterclockwise rotation on a noisy limit cycle, and hence collective coherent oscillatory motion of the global potential $V_G(t)$ occurs. However, when passing a higher threshold D_h^* ($\simeq 16$ μA$\cdot$ms$^{1/2}$/cm^2) incoherent states appear again because noise spoils spiking coherence, as shown in Figs. 1(e) and 1(f) for $D = 30$ μA$\cdot$ms$^{1/2}$/cm^2.

The above incoherence-coherence-incoherence transition may well be described in terms of the order parameter, as in globally coupled chaotic systems.[9–12] For our case, the mean square deviation of the global potential $V_G(t)$ (i.e., time-averaged fluctuations of $V_G(t)$),

$$\mathcal{O} \equiv \overline{(V_G(t) - \overline{V_G(t)})^2}\,, \tag{4}$$

plays the role of an order parameter, where the overbar represents the time averaging. Here, we discard the first time steps of a stochastic trajectory as transients

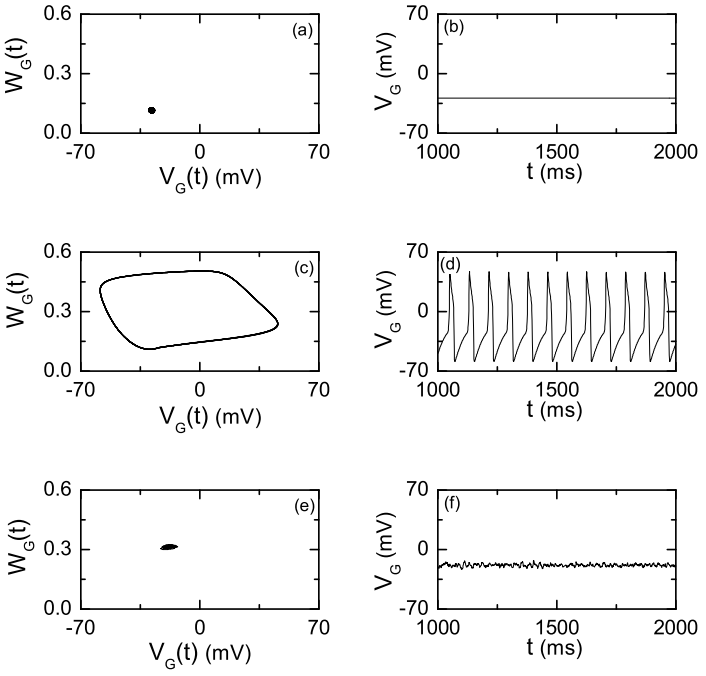

Fig. 1. Incoherence-coherence-incoherence transition for $N = 10^3$ and $J = 50\ \mu\text{A/cm}^2$. Phase portraits of the global state [i.e., lots of $W_G(t)$ versus $V_G(t)$] and the time series of the global potential $V_G(t)$ for (a) and (b) $D = 0.1\ \mu\text{A} \cdot \text{ms}^{1/2}/\text{cm}^2$, (c) and (d) $D = 0.3\ \mu\text{A} \cdot \text{ms}^{1/2}/\text{cm}^2$, and (e) and (f) $D = 30\ \mu\text{A} \cdot \text{ms}^{1/2}/\text{cm}^2$.

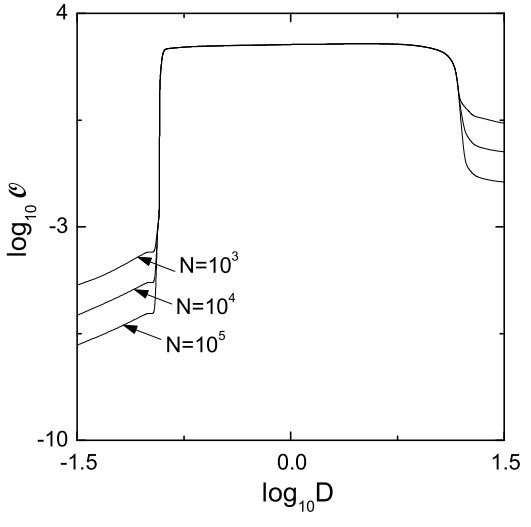

Fig. 2. Plots of the order parameter $\mathcal{O}$ versus the noise intensity D (i.e., plots of $\log_{10}\mathcal{O}$ versus $\log_{10} D$) for $N = 10^3$, 10^4, and 10^5 when $J = 50\ \mu\text{A/cm}^2$. For D_l^* ($\simeq 0.115\ \mu\text{A} \cdot \text{ms}^{1/2}/\text{cm}^2$) $< D < D_h^*$ ($\simeq 16\ \mu\text{A} \cdot \text{ms}^{1/2}/\text{cm}^2$), coherent states exist (i.e., stochastic spiking coherence occurs).

during 10^3 ms, and then we numerically compute $\mathcal{O}$ by following the stochastic trajectory for 10^4 ms when $N = 10^3$, 10^4, and 10^5. For the coherent (incoherent) state, the order parameter $\mathcal{O}$ approaches a nonzero (zero) limit value in the thermodynamic limit of $N \to \infty$. Figure 2 shows a plot of the order parameter versus the noise intensity. For $D < D_l^*$, the order parameter $\mathcal{O}$ tends to zero as $N \to \infty$, and hence incoherent states exist. However, when passing the lower threshold D_l^*, a coherent transition occurs because of a constructive role of noise to stimulate coherence between noise-induced spikings. Thus, stochastic spiking coherence occurs in a large range of intermediate values of noise intensity. However, for $D > D_h^*$ the order parameter $\mathcal{O}$ goes to zero as $N \to \infty$, and hence incoherent states appear as D passes the higher threshold D_h^* due to a destructive role of noise to spoil the spiking coherence.

Finally, we characterize the degree of stochastic spiking coherence (occurring in the coherent regime) in terms of a coherence measure. Figures 3(a1)–3(a5) show phase portraits of the global and local output signals in the coherent regime. Since our neural network is globally coupled, any local neuron may be a representative one. By comparing the global and local phase portraits, we obtain qualitative information about the degree of stochastic spiking coherence. For an optimal noise intensity D^* ($\simeq 0.3\ \mu\text{A} \cdot \text{ms}^{1/2}/\text{cm}^2$), the global state exhibits a collective motion on a gray limit cycle, as shown in Fig. 3(a2). For this optimal case, the degree of stochastic spiking coherence seems to be maximal because the gray limit cycle coincides nearly with the black limit cycle of the first local state. However, as

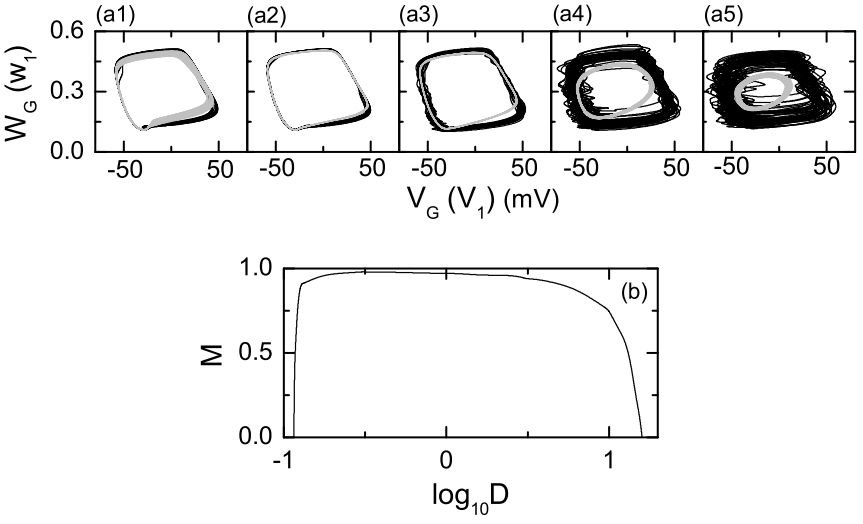

Fig. 3. Phase portraits and coherence measure for $N = 10^3$ and $J = 50\ \mu\text{A/cm}^2$. Gray (black) limit cycles of the global (1st local) state for (a1) $D = 0.13\ \mu\text{A} \cdot \text{ms}^{1/2}/\text{cm}^2$, (a2) $D = 0.3\ \mu\text{A} \cdot \text{ms}^{1/2}/\text{cm}^2$, (a3) $D = 3\ \mu\text{A} \cdot \text{ms}^{1/2}/\text{cm}^2$, (a4) $D = 10\ \mu\text{A} \cdot \text{ms}^{1/2}/\text{cm}^2$, and (a5) $D = 13\ \mu\text{A} \cdot \text{ms}^{1/2}/\text{cm}^2$. (b) Plot of coherence measure M versus $\log_{10} D$.

D is increased from D^* the size of the global gray limit cycle decreases, and the width of the local black limit cycle increases because of fluctuations of local output signals. Similarly, as D is decreased from D^*, the average size of the global limit cycle decreases and its width increases due to fluctuations. In this way, as D is deviated from D^*, the degree of stochastic spiking coherence (i.e., the degree of "resemblance" of the global output signal to the local output signal) decreases. Such degree of stochastic spiking coherence may be quantified by a measure M defined by[17,18]

$$M \equiv \frac{\sqrt{\mathcal{O}}}{\frac{1}{N}\sum_{i=1}^{N}\sqrt{\overline{(V_i(t)-\overline{V_i(t)})^2}}}\,. \tag{5}$$

This coherence measure M is just the ratio between the standard deviation (i.e., the root-mean-square deviation) of the global potential $V_G(t)$ and the population average over each neuron's standard deviation of local potential V_i (i.e., M reflects the degree of "resemblance" of the global potential to the local potential). For the case of a coherent state, $0 < M \leq 1$, while $M = 0$ in the case of an incoherent state. Here, we numerically compute M by following the stochastic trajectory during 200 oscillations of $V_G(t)$ after a transient process of 10^3 ms when $N = 10^3$. Figure 3(b) shows the plot of M versus the noise intensity. As D is increased from the lower threshold D_l^*, M increases dramatically at first, indicating the onset of coherence, then a wide plateau with nearly constant large M is followed, but for large D, M decreases due to the destructive role of noise to spoil the spiking coherence. Thus, stochastic spiking coherence with large M becomes stable over a large range of intermediate noise intensity.

3. Summary

We have numerically investigated stochastic spiking coherence in a large population of globally coupled subthreshold ML neurons by varying the noise intensity D. As D passes a lower threshold, a coherent transition occurs and then stochastic spiking coherence occurs. However, when passing a higher threshold, a transition from a coherent to an incoherent state takes place because noise spoils spiking coherence for large D. This incoherence-coherence-incoherence transition is well-described in terms of the order parameter. In the coherent regime, we also characterize the degree of stochastic spiking coherence in terms of a coherence measure M which reflects the degree of "resemblance" of the global potential to the local potential. Thus, stochastic spiking coherence with large M has been found to occur over a large range of intermediate noise intensity through competition between the constructive and the destructive roles of noise. Finally, we note that stochastic spiking coherence might be an origin for synchronous brain rhythms in the noisy environment which are correlated with brain function of encoding sensory stimuli.

Acknowledgments

This work was supported by the Korea Research Foundation funded by the Korean Government (MOEHRD) (KRF-2005-037-H00017).

References

1. G. Buzsáki, *Rhythms of the Brain* (Oxford University Press, New York, 2006).
2. C. M. Gray, *J. Compu. Neurosci.* **1**, 11 (1994).
3. X.-J. Wang, in *Encyclopedia of Cognitive Science*, ed. L. Nadel (MacMillan, London, 2003), pp. 272–280.
4. L. Gammaitoni, P. Hänggi, P. Jung and F. Harchesoni, *Rev. Mod. Phys.* **70**, 223 (1998).
5. B. Lindner, J. Garcia-Ojalvo, A. Neiman and L. Schimansky-Geier, *Phys. Rep.* **392**, 321 (2004).
6. C. Morris and H. Lecar, *Biophys. J.* **35**, 193 (1981).
7. J. Rinzel and B. Ermentrout, in *Methods in Neural Modeling: From Ions to Networks*, eds. C. Koch and I. Segev (MIT Press, Cambridge, 1998), p. 251.
8. K. Tsumoto, H. Kitajima, T. Yoshinaga, K. Aihara and H. Kawakami, *Neurocomputing* **69**, 293 (2006).
9. S.-J. Baek and E. Ott, *Phys. Rev. E* **69**, 066210 (2004).
10. D. Topaj, W.-H. Kye and A. Pikovsky, *Phys. Rev. Lett.* **87**, 074101 (2001).
11. A. S. Pikovsky, M. G. Rosenblum and J. Kurths, *Europhys. Lett.* **34**, 165 (1996).
12. H. Sakaguchi, *Phys. Rev. E* **61**, 7212 (2000).
13. The values of the parameters are the same as those in Ref. 7 except for the membrane capacitance C; more coherent states seem to appear for smaller C.
14. A. L. Hodgkin, *J. Physiol.* **107**, 165 (1948).
15. E. M. Izhikevich, *Int. J. Bifurc. Chaos* **10**, 1171 (2000).
16. M. San Miguel and R. Toral, in *Instabilities and Nonequilibrium Structures VI*, eds. J. Martinez, R. Tiemann and E. Tirapegui (Kluwer Academic Publisher, Dordrecht, 2000), p. 35.
17. D. Golomb and J. Rinzel, *Physica D* **72**, 259 (1994).
18. D. Hansel and G. Mato, *Neural Compu.* **15**, 1 (2003).